Table IX. Atomic Charges for the Sulfide Nonacarbonyl Clusters[a]

cluster	atomic charges M	S	H
$SCo_3(CO)_9$			
Co	0.129-	0.130-	
$SFeCo_2(CO)_9$			
Co	0.141-	0.176-	
Fe	0.078+		
$SHFe_2Co(CO)_9$			
Co	0.134-	0.152-	0.141-
Fe	0.028-		
$SH_2Fe_3(CO)_9$			
Fe	0.046-	0.166-	0.141-
Fe*	0.062+		
$SH_2Ru_3(CO)_9$			
Ru	0.174+	0.497-	0.279-
Ru*	0.434+		
$S_2Fe_3(CO)_9$			
Fe(1)	0.005-	0.200-	
Fe(2)	0.075-		
Fe(3)	0.141+		

[a] An asterisk denotes that the metal is the unique one.

sufficiently large. The orbitals lying along the cluster's M-M internuclear axis are mainly derived from the e_g-like orbitals of the $M(CO)_3$ fragments.[34] These form a bonding set, which is totally occupied, and an antibonding unoccupied set. The M-H-M interactions are more intricate as suggested by the overlap populations in Table VIII. The M-M axis, bridged by H, has a decreased d-d overlap when compared to the nonbridged M-M interactions. The M(d)-H (M = Fe, Ru) overlap populations suggest that there are substantial disruptions of the M-M bond by a bridging H atom. The M-M bonds not bridged by H in these clusters are predominantly e_g-like in character. The loss of M-M e_g-like character to form M-H-M interactions is observed in both the calculations and the PE spectra. Interestingly the t_{2g}-like overlap populations go positive in the H-bridged FeCo clusters. It is this interaction, enhanced by a second H bridge, that is responsible for the short M-M bond in $H_2Os_3(CO)_{10}$.[32e]

Theoretically, the H atoms may interact with the metals directly by forming bonding and antibonding orbitals or indirectly by withdrawing charge.[35] The negative charge accumulated by H stabilizes the metal levels and results in a hydridic hydrogen. Recently, the geometrical[36] and theoretical[33] comparison between the isoelectronic $(\mu_3\text{-}CCH_3)Co_3(CO)_9$ and $(\mu_3\text{-}CCH_3)Fe_3(\mu\text{-}H)_3(CO)_9$ clusters suggests that the H atoms act like hydridic ligands. The gross charges for the H atoms in the Fe-H-Fe and Ru-H-Ru sulfides are 0.141- and 0.279-, respectively (Table IX). The S ligand also bears a negative charge (Table IX). As mentioned previously, the S 3p orbital directed toward the center of the cluster donates less electron density than those that are tangential. This important distinction arises because the inward-directed orbital interacts strongly with a t_{2g}-like metal orbital, which is sufficiently stabilized by the carbonyls that the M-S antibonding counterpart is also filled. Here again we see the participation of the t_{2g}-like orbitals, which are usually thought to be nonbonding.[37]

Acknowledgment is made to the Robert A. Welch Foundation (Grant A-648) and the National Science Foundation (Grant CHE 79-20993) for support of this work.

Registry No. 1, 22364-22-3; $SCo_3(CO)_9$, 35260-81-2; $SHFe_2Co(CO)_9$, 78547-58-7; $SH_2Fe_3(CO)_9$, 78547-62-3; $S_2Fe_3(CO)_9$, 22309-04-2; $SH_2Ru_3(CO)_9$, 32574-35-9; $SH_2OS_3(CO)_9$, 38979-82-7.

(34) Elian, M.; Hoffmann, R. *Inorg. Chem.* **1975**, *14*, 1058.

(35) (a) Hoffmann, R. *Acc. Chem. Res.* **1971**, *4*, 1. (b) Surjan, P. R.; Mayer, I.; Kertesz, M. *J. Chem. Phys.* **1982**, *77*, 2454.

(36) Wong, K. S.; Haller, K. J.; Dutta, T. K.; Chipman, D. M.; Fehlner, T. P. *Inorg. Chem.* **1982**, *21*, 3197.

(37) (a) Hoffmann, R. *Science (Washington, D.C.)* **1981**, *211*, 995 and references therein. (b) Hoffmann, R. *Angew. Chem., Int. Ed. Engl.* **1982**, *21*, 711 and references therein.

Contribution from the Division of Chemical and Physical Sciences, Deakin University, Waurn Ponds 3217, Victoria, Australia

Electrochemical-Electron Spin Resonance Investigation of Reactions of 17-Electron Iron Carbonyl Radical Cation Complexes

R. N. BAGCHI, A. M. BOND,* C. L. HEGGIE, T. L. HENDERSON, E. MOCELLIN, and R. A. SEIKEL

Received November 24, 1982

In situ electrochemical oxidation of $Fe(CO)_3(PPh_3)_2$ in dichloromethane in the cavity of an electron spin resonance (ESR) spectrometer, having variable-temperature capabilities and a microprocessor-based data acquisition system, enables the formation and decay of the 17-electron cation radical $[Fe(CO)_3(PPh_3)_2]^+$ to be studied. Electrolysis at platinum electrodes shows that $[Fe(CO)_3(PPh_3)_2]^+$ is relatively stable in noncoordinating solvents in the absence of oxygen and light. At silver and mercury electrodes, $[Fe(CO)_3(PPh_3)_2]^+$, while also being the stable product of electrolysis, is generated via silver and mercury intermediates, which are also light sensitive. $[Fe(CO)_3(PPh_3)_2]^+$ reacts with acetone (or acetonitrile) in a second-order process to produce transient solvent-substituted cation radical species that participate in a series of reactions to produce $Fe(CO)_3(PPh_3)_2$ and iron(II) compounds. These reactions appear to parallel those reported previously with anionic ligands. The reaction of $[Fe(CO)_3(PPh_3)_2]^+$ with PPh_3, $AsPh_3$, $SbPh_3$, $Fe(CO)_4PPh_3$, $Fe(CO)_3(AsPh_3)_2$, $Fe(CO)_4AsPh_3$, $Fe(CO)_3(SbPh_3)_2$, or $Fe(CO)_4SbPh_3$ in dichloromethane is stoichiometric and rapid, producing $Fe(CO)_3(PPh_3)_2$ and other species. Evidence for dimer formation as an intermediate is inferred from the ESR data with some of these reactions. Subsequent radical and molecular reactions lead to identification of $Fe(CO)_3(PPh_3)_2Cl$ at -35 °C, with chloride being obtained from the solvent dichloromethane.

The chemistry of zerovalent iron carbonyl moieties has been studied extensively.[1,2] The chemistry of iron(II) carbonyl complexes has also been examined in some depth.[1-4] The zerovalent complexes are predominantly five-coordinate, while

0020-1669/83/1322-3007$01.50/0

the oxidation state II species usually are six-coordinate. Both of these classes of compounds are relatively stable and formally have 18-electron electronic configurations, thereby obeying the effective atomic number rule.[1]

Paramagnetic, formally iron(I) 17-electron species may be formed as intermediates, in the chemical oxidation of the zerovalent compounds. However, generally these have been undetected, and iron(II) rather than iron(I) compounds are isolated from chemical oxidation reactions.[4]

Electrochemical oxidation of iron carbonyl complexes has produced some conflicting data.[5] Results indicate that stable 17-electron cation radicals, e.g. $[Fe(CO)_3(PPh_3)_2]^+$, exist, but considerable electrode and solvent dependence has been noted. For example, cyclic voltammograms at mercury electrodes are frequently very different from those at platinum. At mercury electrodes, reversible one-electron oxidation has been reported, whereas at platinum, for some complexes and in solvents such as acetonitrile, no evidence of stable 17-electron cations is found. Connelly et al.[6-8] have examined several aspects of the electrochemical and chemical oxidation of iron carbonyl complexes. They have isolated the radical cation $[Fe(CO)_3(PPh_3)_2]^+$ as a hexafluorophosphate salt.[7,8] Some electron spin resonance, ESR, data obtained after chemical oxidation of tricarbonyl species, $Fe(CO)_3L_2$ (L = arsenic or phosphorus ligands), indicate that a range of other cation radicals may be reasonably stable. However, some data appear to be in conflict. Thus, these authors provide electrochemical data that imply that $[Fe(CO)_3(AsPh_3)_2]^+$ has no stability on the electrochemical time scale; i.e., oxidation of $Fe(CO)_3(AsPh_3)_2$ is chemically irreversible.[8] In contrast, chemical oxidation data coupled with ESR data reported in the same paper suggest that $[Fe(CO)_3(AsPh_3)_2]^+$ is stable on the much longer synthetic time scale. This apparent anomaly, while noted, was not explained by the authors.

In an endeavor to further understand the chemistry and electrochemistry of paramagnetic 17-electron iron carbonyl complexes, we have undertaken a combined electrochemical–ESR investigation of the substituted carbonyl complexes. A variable-temperature ESR–electrochemical cell was employed so that products of electrolysis would be generated directly in the ESR cavity and if necessary stabilized by the use of low temperatures. For studies of fast reactions, a microprocessor-based data acquisition system was interfaced to the ESR spectrometer.[9]

Experimental Section

Synthesis of Compounds. *trans*-$Fe(CO)_3(PPh_3)_2$ was prepared by refluxing stoichiometric amounts of triiron dodecacarbonyl, $Fe_3(CO)_{12}$, and triphenylphosphine, PPh_3, in dry tetrahydrofuran for 30 min. After partial evaporation of the solvent, yellow crystals were obtained on cooling, which were purified by recrystallization from dichloromethane/hexane. Column chromatography of the recrystallized material, on alumina, using dichloromethane as eluent, separated $Fe(CO)_3(PPh_3)_2$ from $Fe(CO)_4PPh_3$.

The compound was stored in a vacuum desiccator at 0 °C to slow down the decomposition.

The purity of the compound was ascertained by infrared spectroscopy (single carbonyl band) at 1879 cm^{-1},[5-8] microanalytical data, and polarographic data (no oxidation of mercury in presence of triphenylphosphine).

trans-$[Fe(CO)_3(PPh_3)_2]PF_6$ was synthesized by the method described by Baker et al.[8] This compound was stored at liquid-nitrogen temperatures and used within 24 h of preparation.

Other chemicals and solvents (chromatographic grade) were used as supplied by the manufacturer. Supporting electrolytes were recrystallized prior to use.

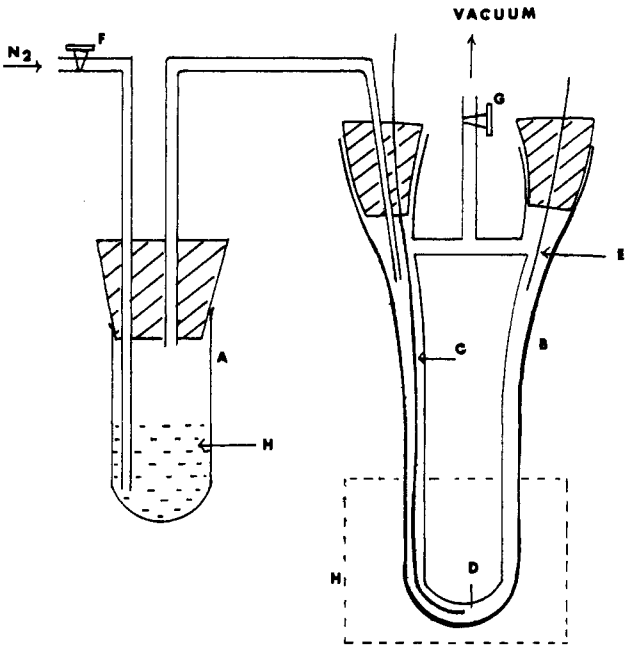

Figure 1. ESR–electrochemical cell with deoxygenation unit: (A) nitrogen bubbler; (B) ESR–electrochemical cell; (C) working electrode; (D) reference electrode; (E) auxiliary electrode; (F, G) valves; (H) microwave cavity.

Electrochemical–ESR Equipment. The ESR spectra were obtained with a reflection type X-band system employing 100-kHz modulation for phase lock-in amplification. A Varian biological microwave cavity (E 231) of unloaded Q of ≈7000 was used. The loaded Q was approximately 3000 when the electrolytic cell (with the sample and the electrodes) was inserted into the cavity. With a temperature controller (DELTRON) employing liquid nitrogen for cooling the sample cell, it was possible to vary the temperature from +30 to −150 °C with a stability of ±1 °C.

A Motorola M 6800 microprocessor-based data acquisition system was interfaced with the ESR spectrometer for signal averaging and transient recording. The details of the system are described elsewhere.[9] With use of a 50-Hz magnetic field sweep, a complete spectrum could be acquired within 10 ms.

In situ electrolysis was carried out in a variable-temperature ESR–electrolytic cell (Figure 1) using platinum or silver working electrodes.

Before the introduction of the sample, the cell was alternately evacuated and then purged by nitrogen, which was passed through the sample solution in the bubbler. After 10 min of purging, the bubbler was tipped and the sample was forced into the cell by the pressure gradient between A and B (see Figure 1). A slightly higher than ambient nitrogen pressure ensures that the sample remains relatively oxygen free during and after transfer to the ESR cell. The amount of sample exposed to microwaves inside the cavity is small even though the internal diameter of the active part of the cell is approximately 10 times the thickness of a conventional flat cell. The cell design achieves three important objectives: (a) improvement of the loaded Q of the cavity and consequent increase of ESR sensitivity, (b) an increase in the dc conductivity of the sample, and (c) insertion of the cell inside a rectangular variable-temperature dewar. The higher conductivity overcomes one of the major problems in electrochemistry

(1) F. A. Cotton and G. Wilkinson, "Advanced Inorganic Chemistry", 3rd ed., Interscience, New York, 1972.
(2) E. A. Koesner von Gustorf, F.-W. Grevels, and I. Fischler, "The Organic Chemistry of Iron", Academic Press, New York, 1978, and references cited therein.
(3) C. A. McAuliffe, Ed., "Transition Metal Complexes of Phosphorus, Arsenic and Antimony Ligands", Macmillan, New York, London, and Basingstoke, 1973.
(4) W. Hieber and J. Muschi, *Chem. Ber.*, **98**, 3931 (1965).
(5) S. W. Blanch, A. M. Bond, and R. Colton, *Inorg. Chem.*, **20**, 755 (1981), and references cited therein.
(6) N. G. Connelly and K. R. Somers, *J. Organomet. Chem.*, **113**, C39 (1976).
(7) P. K. Baker, K. Broadley, and N. G. Connelly, *J. Chem. Soc., Chem. Commun.*, 775 (1980).
(8) P. K. Baker, N. G. Connelly, B. M. R. Jones, J. P. Maher, and K. R. Somers, *J. Chem. Soc., Dalton Trans.*, 579 (1980).
(9) J. E. Anderson, R. N. Bagchi, A. M. Bond, H. B. Greenhill, T. L. Henderson, F. L. Walter, *Am. Lab. (Fairfield Conn.)*, **13** (2), 21–32 (1981).

when low-conductivity aprotic solvents (e.g. CH_2Cl_2) are used, i.e. ohmic resistance compensation.

For kinetic studies, the paramagnetic species were generated electrochemically in the cell; when a measurable ESR spectrum was observed, the electrolysis was stopped and the complete spectrum was stored in the transient recorder at preset intervals. The stored spectra were subsequently output to a chart recorder. Some electrogenerated species were not stable enough at room temperature for observation. For these the temperature had to be lowered. Silver, platinum, and mercury working electrodes were used. For mercury a conventional room-temperature flat cell had to be employed.

Electrolysis and voltammetric experiments were undertaken with a PAR Model 173 potentiostat/galvanostat and Model 175 universal programmer. A Ag/AgCl reference electrode (saturated, LiCl in CH_2Cl_2) and platinum-wire auxiliary electrodes were used for all electrochemical experiments. Working electrodes are as stated in the text.

Results and Discussion

(a) Electrochemical Oxidation of $Fe(CO)_3(PPh_3)$ and Reduction of $[Fe(CO)_3(PPh_3)_2]^+$ in Dichloromethane. The electrochemical oxidation of $Fe(CO)_3(PPh_3)_2$ has been examined previously. However, while it would be presumed that $[Fe(CO)_3(PPh_3)_2]^+$ could be reduced to $Fe(CO)_3(PPh_3)_2$, this important aspect of the electrochemistry has yet to be reported. Complete characterization of the $[Fe(CO)_3(PPh_3)_2]^+/Fe(CO)_3(PPh_3)_2$ redox couple requires that these experiments be undertaken.

Dc polarograms for oxidation of $Fe(CO)_3(PPh_3)_2$ in CH_2Cl_2 (0.1 M Bu_4NClO_4) at 20 °C show characteristics of adsorption.[5] Use of the limiting current, at concentrations less than 10^{-4} M where adsorption effects are minimal, and the Ilkovic equation indicates that this complex has a diffusion coefficient of approximately 10^{-5} cm^2 s^{-1}. Dc polarograms for reduction of $[Fe(CO)_3(PPh_3)_2]^+$ produced large maxima and concentration-dependent behavior characteristic of strong adsorption. The implication that mercury complex formation may be associated with the redox process[5] seems to be substantiated.

Cyclic voltammograms for oxidation of $Fe(CO)_3(PPh_3)_2$ at platinum electrodes were well-defined with behavior characteristics of a quasi-reversible one-electron oxidation step. Using variable scan rates between 20 and 500 mV s^{-1}, theory based on digital simulation,[10] equal diffusion coefficients for $Fe(CO)_3(PPh_3)_2$ and $[Fe(CO)_3(PPh_3)_2]^+$, a charge-transfer coefficient of 0.5, and a one-electron oxidation leads to a calculated value of approximately 10^{-3} cm s^{-1} for the heterogeneous charge-transfer rate constant, k_s, for the electrode process

$$Fe(CO)_3(PPh_3)_2 \overset{k_s}{\rightleftharpoons} [Fe(CO)_3(PPh_3)_2]^+ + e^- \quad (1)$$

at platinum electrodes. An E° value of 0.46 ± 0.20 V vs. Ag/AgCl (CH_2Cl_2, satd LiCl) was calculated from the comparison of theory and experiment. Reduction of $[Fe(CO)_3(PPh_3)_2]^+$ at platinum electrodes produced a quasi-reversible cyclic voltammogram with a calculated E° value of 0.48 ± 0.20 V vs. Ag/AgCl (CH_2Cl_2, satd LiCl). Equation 1 therefore seems to be an adequate description of the electrode process at platinum electrodes, but not at mercury electrodes.

(b) Electrolysis in the ESR Cavity at Platinum Electrodes in Dichloromethane. In dichloromethane (0.1 M Bu_4NClO_4), electrolysis of yellow *trans*-$Fe(CO)_3(PPh_3)_2$ at platinum electrodes at 20 °C inside an ESR cavity produces a triplet in the ESR spectrum with relative intensities of 1:2:1 (Figure 2a), $\langle g \rangle = 2.052$, $\langle A \rangle = 1.95$ mT, and line width (ΔB) = 0.82 mT. Essentially the same ESR spectrum is produced over the temperature range of −50 to +20 °C. This spectrum is, within the limit of experimental error, identical with that obtained from a dichloromethane solution of the green, chemically synthesized *trans*-$[Fe(CO)_3(PPh_3)_2][PF_6]$ salt. Data are also similar to those provided elsewhere[5,8] when the cation radical was produced in experiments undertaken outside the ESR spectrometer cavity.

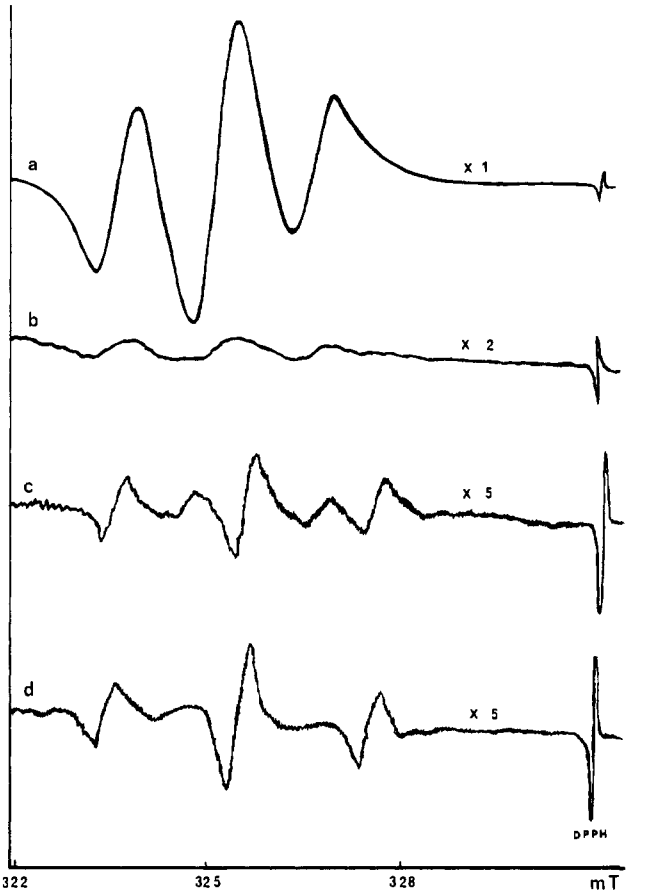

Figure 2. Changes observed in the ESR spectrum when free ligands (e.g. $AsPh_3$, PPh_3, $SbPh_3$, etc.) are mixed with $[Fe(CO)_3(PPh_3)_2]^+$ at −35 °C: (a) before mixing; (b) 1 min after mixing; (c) 10 min after mixing; (d) 20 min after mixing.

The rate of decay of $[Fe(CO)_3(PPh_3)_2]^+$ generated electrochemically in CH_2Cl_2 (0.1 M Bu_4NClO_4) was critically dependent on the presence of water, oxygen, or light. Irrespective of the concentration of water or oxygen, ESR monitoring of the rate of decay always produced first-order kinetics. After careful removal of oxygen (nitrogen bubbling) and water (molecular sieves) combined with sealing of the ESR tube and careful protection from light, a first-order rate constant of (5.0 ± 0.5) × 10^{-4} s^{-1} was obtained at 20 °C. Deliberate addition of water, oxygen, or light produced a far more rapid rate of decay. At −50 °C, the half-life was greater than 1 day. A small quantity of *trans*-$Fe(CO)_3(PPh_3)_2$ complex was observed as a product of decomposition (infrared evidence) along with an unidentified, non-carbonyl-containing, brown sediment-like material.

The decomposition of the cation radical in (water-, oxygen-, and light-free) CH_2Cl_2 is probably a pseudo-first-order reaction involving the solvent CH_2Cl_2 and chloride abstraction:

$$[Fe(CO)_3(PPh_3)_2]^+ \xrightarrow{CH_2Cl_2 \text{ (very slow)}} Fe(CO)_3(PPh_3)_2Cl \rightarrow \text{products} \quad (2)$$

The structure of the complex $Fe(CO)_3(PPh_3)_2Cl$ has yet to be unambiguously clarified,[8,11] with either the 19-electron

(10) S. W. Feldberg, "Electroanalytical Chemistry", Vol. 3, A. J. Bard, Ed., Marcel Dekker, New York, 1969, pp 199–296.

(11) P. K. Baker, K. Broadley, and N. G. Connelly, *J. Chem. Soc., Dalton Trans.*, 471 (1982).

species containing a direct Fe–Cl bond or a 17-electron complex containing a chloroacyl group being proposed.

Dichloromethane and related solvents are frequently associated with chloride abstraction and redox reactions and may contain chloride impurities.[12,13] The inevitable presence of traces of oxygen, water, and light introduces uncertainties into the interpretation, and parallel reaction pathways may be occurring. $Fe(CO)_3(PPh_3)_2Cl$ is relatively reactive[8] and is expected to produce $Fe(CO)_3(PPh_3)_2$ and iron(II) products. Eighteen-electron iron(0) or iron(II) compounds are themselves not completely stable[13-15] so the very small yield of $Fe(CO)_3(PPh_3)_2$ is to be expected with this mechanism.

(c) Electrolysis in the ESR Cavity at Silver or Mercury Electrodes in Dichloromethane. Chemical oxidation of $Fe(CO)_3(PPh_3)_2$ with silver perchlorate in CH_2Cl_2 appears to involve silver intermediates.[8] In the presence of sunlight, the appearance of green $[Fe(CO)_3(PPh_3)_2]^+$ is rapid while in the dark it is relatively slow. Therefore, we find the rate of generation of the cation radical from the silver intermediate to be light sensitive. The reaction proposed is

$$Ag^+ + 2Fe(CO)_3(PPh_3)_2 \rightleftharpoons [Ag(Fe(CO)_3(PPh_3)_2)_2]^+ \xrightarrow{h\nu} Ag\downarrow + [Fe(CO)_3(PPh_3)_2]^+ + Fe(CO)_3(PPh_3)_2 \quad (3)$$

Linear silver(I) complexes are well-known in inorganic chemistry.[16-18]

In view of the silver intermediate found in the chemical reaction, the question arises as to whether electrochemical oxidation at silver or mercury electrodes occurs via silver or mercury intermediates. ESR data provide evidence that the same radical species is produced at silver and mercury electrodes as was the case at platinum, i.e. $[Fe(CO)_3(PPh_3)_2]^+$. However, at both silver and mercury electrodes the ESR signal does not appear for some time after the potential is stepped to where current flows. Furthermore, the magnitude of the signal continues to increase for a finite period after switching off the potentiostat. By contrast, the ESR signal at platinum electrodes is observed immediately the potential is switched to where current flows and decays after switching off the potentiostat as diffusion of the cation radical away from the electrode occurs. The contrasting behavior at platinum vs. silver or mercury electrodes provides strong evidence that diamagnetic mercury and silver complexes are formed at the electrode surface prior to generation of the radical cations. This is consistent with the hypothesis of a mercury-stabilized cation radical influencing the electrochemical behavior.[5]

(d) Electrolysis in the ESR Cavity in Acetone and Acetonitrile. In acetone (0.1 M Bu_4NClO_4) electrochemical–ESR data at platinum, silver, or mercury electrodes indicate that $[Fe(CO)_3(PPh_3)_2]^+$ is relatively reactive compared to the situation in CH_2Cl_2. ESR parameters in acetone were as follows: $\langle g \rangle = 2.052$, $\langle A \rangle = 1.95$ mT, line width $(\Delta B) = 0.82$ mT. The rate of decay obeys the theory for first-order kinetics in acetone. However, using mixtures of acetone and dichloromethane shows that the decay of the signal is actually a second-order process (Figure 3). A second-order rate constant of $(3.5 \pm 0.5) \times 10^{-3}$ M^{-1} s^{-1} was obtained at 20 °C

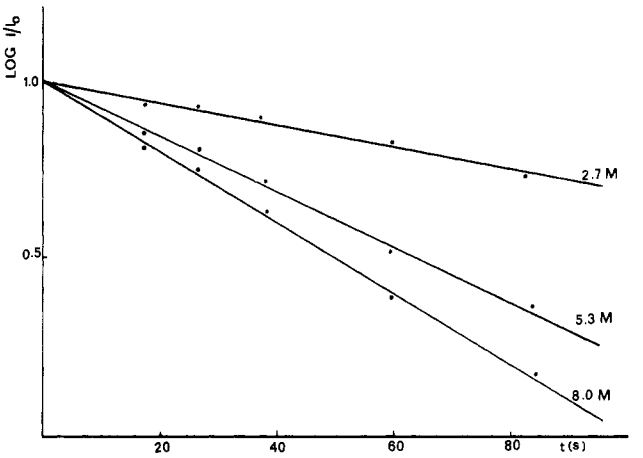

Figure 3. Variation of ESR signal intensity with time for different concentrations of acetone added to dichloromethane. Pseudo-first-order rate constants are 0.010, 0.020, and 0.027 s^{-1} for acetone concentrations of 2.7, 5.3, and 8.0 M, respectively, corresponding to a second-order rate constant of 4×10^{-3} L mol^{-1} s^{-1}.

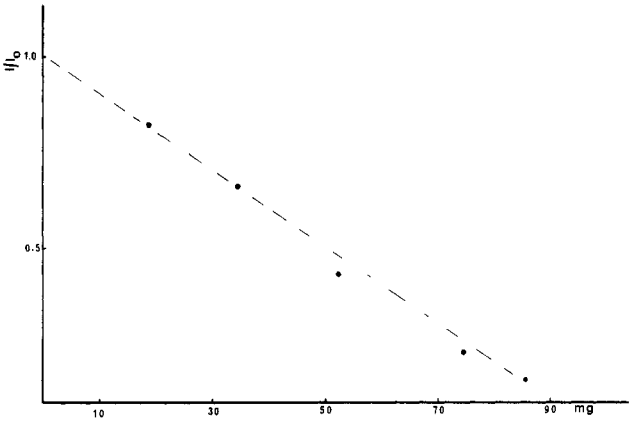

Figure 4. Variation of ESR signal intensity of $[Fe(CO)_3(PPh_3)_2]^+$ with the addition of PPh_3. Intensities were measured immediately after this addition.

for the decay process in acetone. Similar experiments in acetonitrile showed that the rate of decay was much faster than in acetone. The solvent stability order dichloromethane > acetone > acetonitrile parallels that of the coordinating ability of the solvents. The electrochemically reversible behavior at mercury electrodes in acetonitrile compared with the chemically irreversible response observed at platinum[5] is now confirmed to arise from the enhanced stability of the mercury complex formed at the electrode surface toward attack by coordinating solvents. $Fe(CO)_3(PPh_3)_2$ was identified as a product resulting from addition of solvent to $[Fe(CO)_3(PPh_3)_2]^+$, as was triphenylphosphine, triphenylphosphine oxide, and carbon monoxide.

(e) Electrolysis in the ESR Cavity Followed by Addition of Other Ligands and Iron Carbonyl Complexes. Electrolysis of $Fe(CO)_3(PPh_3)_2$ at platinum electrodes in CH_2Cl_2 (0.1 M Bu_4NClO_4) at 20 °C produces an ESR signal for $[Fe(CO)_3(PPh_3)_2]^+$ as described above. Addition of $Fe(CO)_3(PPh_3)_2$ did not alter the ESR signal of the cation radical. However, each of PPh_3, $AsPH_3$, $SbPH_3$, $Fe(CO)_4AsPh_3$, $Fe(CO)_4SbPh_3$, $Fe(CO)_4$, $Fe(CO)_3(AsPh_3)_2$, and $Fe(CO)_3(SbPh_3)_2$ caused a decrease in the signal (Figure 4). At 20 °C and with equal concentrations of $[Fe(CO)_3(PPh_3)_2]^+$ and added chemical, no ESR signal is detected. At low temperatures, disappearance of the cation radical signal occurs as at 20 °C. However, at or below −35 °C, a new signal appears after a period of time. ESR data for the new triplet appearing after decay of the $[Fe(CO)_3(PPh_3)_2]^+$ spectrum are as follows:

(12) O. J. Scherer and H. Jungmann, *J. Organomet. Chem.*, **208**, 153 (1981).
(13) G. Bellachioma, G. Cardaci, and G. Reichenbach, *J. Organomet. Chem.*, **221**, 291 (1981).
(14) M. A. Schroeder and M. S. Wrighton, *J. Organomet. Chem.*, **128**, 345 (1977), and references cited therein.
(15) G. L. Swartz and R. J. Clark, *Inorg. Chem.*, **19**, 3191 (1980), and references cited therein.
(16) P. K. Baker, K. Broadley, N. G. Connelly, B. A. Kelly, M. D. Kitchen, and P. Woodward, *J. Chem. Soc., Dalton Trans.* 1710 (1980), and references cited therein.
(17) E. C. Alyea, S. A. Dias, and S. Stevens, *Inorg. Chim. Acta*, **44**, L203 (1980).
(18) H. Jendralla, *Angew. Chem., Int. Ed. Engl.*, **19**, 1032 (1980).

$\langle g \rangle$ = 2.046, $\langle A \rangle$ = 2.50 mT, line width (ΔB) = 0.38 mT. For all species added, the low-temperature signal observed after a period of absence of any ESR signal is, within the limit of experimental error, identical with that reported for $Fe(CO)_3(PPh_3)_2Cl$.[8]

Infrared monitoring of the reaction between chemically synthesized $[Fe(CO)_3(PPh_3)_2]^+$ and triphenylphosphine ligands or iron carbonyl complexes in CH_2Cl_2 at 20 °C provided strong evidence that 18-electron tricarbonyl species were being formed as the final product. Reaction yields were always less than 75% and extremely variable, with light and oxygen being important. In some arsenic and stibine reactions, generation of iron tetracarbonyl species was also evident. With time, the tetracarbonyl complexes were converted to tricarbonyl species, so that tetracarbonyl complexes may have been intermediate in many of the reactions. Deliberate addition of excess ligand speeded up the rate of conversion of tetracarbonyl complexes to the tricarbonyl forms. Evolution of carbon monoxide accompanied all of these reactions. Additionally, triphenylphosphine oxide was frequently observed as a product, but yields were not reproducible. Addition of PPh_3 to $[Fe(CO)_3(PPh_3)_2]^+$ in an electrochemical cell led to the observation of the reduction response for $[Fe(CO)_3(PPh_3)_2]^+$ being converted into the oxidation response expected for $Fe(CO)_3(PPh_3)_2$ with an approximately 70% yield. The solution color changed from green to yellow in the course of this experiment. The presence of triphenylphosphine oxide, can also be detected after this reaction.

The above data considered in combination lead to the conclusion that five-coordinate 17-electron substituted iron(I) carbonyl complexes are extremely reactive, with parallel reaction paths operative.

(f) Reaction Pathways. Despite the absence of complete reaction descriptions, electrochemical–ESR observations enable some of the contradictory results in the literature to be rationalized. Electrochemical oxidation at mercury electrodes, accompanied by adsorption but leading to apparent observation of stable species such as $[Fe(CO)_3(AsPh_3)_2]^+$, occurs because interaction with mercury (or silver) occurs at the electrode surface to produce "mercury- (or silver-) stabilized" cation radicals.[5] After removal from the electrode surface, these metal complexes break down to form the 17-electron cation radicals. At platinum electrodes, platinum complexes are not formed at the surface, and chemically irreversible behavior attributable to rapid reaction with a solvent such as CH_3CN and/or other species may occur. Chemically reversible behavior at platinum electrodes in CH_2Cl_2 is found with $Fe(CO)_3(PPh_3)_2$ because $Fe(CO)_3(PPh_3)_2^+$ does not react with $Fe(CO)_3(PPh_3)_2$ or the solvent on the electrochemical time scale.

The electrode process at silver and mercury electrodes can therefore be written in the form

$$2Fe(CO)_3(YPh_3)_2 + M \rightarrow [(YPh_3)_2(CO)_3Fe\text{–}M\text{–}Fe(CO)_3(YPh_3)_2]^+ + e^- \qquad M = Ag, Hg;\ Y = P, As, Sb \qquad (4)$$

At the electrode surface, as an adsorbed species $[M(Fe(CO)_3(YPh_3)_2)_2]^+$ is stable, but on ultimate transport back to the bulk solution, as occurs in a long-time-scale controlled-potential electrolysis experiment, subsequent reactions generate M, $[Fe(CO)_3(YPh_3)_2]^+$, and $Fe(CO)_3(YPh_3)_2$. Once the ionic species is removed from the electrode surface and is in the form of the cation radical rather than a metal-stabilized cation, attack by acetone, acetonitrile, PPh_3, $Fe(CO)_3(AsPh_3)_2$, etc. can occur as is the case when the cation radical is generated directly at platinum electrodes.

Reactions of mono- and disubstituted derivatives of iron pentacarbonyl with alkyl halides occur through parallel radical and molecular paths.[13] For example, $Fe(CO)_3(AsPh_3)_2$ reacts with CCl_4 to give $Fe(CO)_2(AsPh_3)_2Cl_2$. This reaction is radical and is affected by light and duroquinone. This mechanism can be related to the reaction between $Fe(CO)_3(PPh_3)_2$ and halogens.[8] The reaction between $Fe(CO)_3(PMe_3)_2$ and MeI forms $Fe(CO)_2(PMe_3)_2(COMe)I$, in which it has been assumed that concerted nucleophilic displacement involving formation of an anionic intermediate occurs.[13] These reactions associated with the 18-electron iron carbonyl complexes seem to have parallels in the reaction pathway associated with reaction of the $[Fe(CO)_3(PPh_3)_2]^+$ species, implying that the 17-electron cation radical is an intermediate in many oxidative addition reactions.

The reaction of halide ion is known to include several steps:[8]

$$Fe(CO)_3(PPh_3)_2^+ + X^- \rightarrow Fe(CO)_3(PPh_3)_2X \qquad (5)$$

$$Fe(CO)_3(PPh_3)_2X + [Fe(CO)_3(PPh_3)_2]^+ \rightarrow [Fe(CO)_3(PPh_3)_2X]^+ + Fe(CO)_3(PPh_3)_2 \qquad (6)$$

$$[Fe(CO)_3(PPh_3)_2X]^+ + X^- \rightarrow Fe(CO)_{4-n}(PPh_3)_nX_2 + CO \text{ or } PPh_3 \qquad (7)$$

The structural formulation of the intermediate as $Fe(CO)_3(PPh_3)X$ may not be correct,[11] but this kind of mechanism is consistent with one of the reaction pathways noted in this work. That is, we observe $Fe(CO)_3(PPh_3)_2$ as a common reaction product as well as evolution of carbon monoxide and loss of triphenylphosphine.

The E° value for the $[Fe(CO)_3(PPh_3)_2]^+/Fe(CO)_3(PPh_3)_2$ couple of approximately 0.46 V vs. Ag/AgCl implies that $[Fe(CO)_3(PPh_3)_2]^+$ is a weak oxidant. A redox reaction with PPh_3 is therefore not unexpected although the mechanism of the reaction is unknown and may occur by catalysis. Identification of triphenylphosphine oxide as a product implies that catalysis by oxygen occurs:

$$[Fe(CO)_3(PPh_3)_2]^+ + 2PPh_3 + {}^1/_2O_2 \rightarrow Fe(CO)_3(PPh_3)_2 + O{=}PPh_3 + \text{products} \qquad (8)$$

This class of reactions is relatively common with carbonyl compounds (see ref 19 for example).

Since $[Fe(CO)_3(PPh_3)_2]^+$ is light-, oxygen-, and moisture-sensitive as well as prone to substitution reactions and redox activity, it is not surprising that a number of parallel reaction pathways exist. In the case of anionic ligands, the charge would appear to enhance the stability of species such as $Fe(CO)_3(PPh_3)_2X$ and $Fe(CO)_2(PPh_3)_2X_2$ as identifiable intermediates and products, respectively. Such species could not be identified in reactions reported in this work. For example, in the reaction of $[Fe(CO)_3(PPh_3)_2]^+$ with acetone or acetonitrile no ESR spectrum corresponding to that observed for the species $Fe(CO)_3(PPh_3)_2S$ (or $Fe(CO)_2(COS)(PPh_3)_2$) (S = solvent) was observed. That is, no paramagnetic 19- (or 17-) electron intermediates were detectable. However, the rate law is second order, and the reaction rate follows the trend expected when coordinating ability of ligand is a driving force. Substitution of acetone and acetonitrile therefore appears to be associated with the rate-determining step. A dimerization step following the formation of the intermediate would also seem an appropriate step leading to formation of 18-electron iron carbonyl complexes and presumably unstable iron(II) species as has been postulated with halide reactions.[11] While there is no evidence enabling distinction between a 17- or 19-electron intermediate, a reaction scheme of the type shown by (9) as well as related ones would be consistent with the observed overall reaction pathway.

(19) D. M. Roundhill, M. K. Dickson, W. S. Dixit, and B. P. Sudha-Dixit, *Adv. Chem. Ser.*, **No. 196**, 291 (1982).

$$[Fe(CO)_3(PPh_3)_2]^+ + \text{acetone} \longrightarrow [Fe(CO)_2(PPh_3)_2(\text{acetone})]^+ + CO$$

$$[Fe(CO)_2(PPh_3)_2(\text{acetone})]^+ + [Fe(CO)_3(PPh_3)_2]^+ \longrightarrow$$

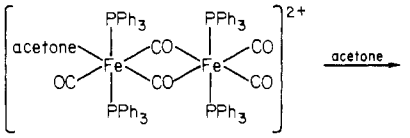

$$[Fe(CO)_2(PPh_3)_2(\text{acetone})_2]^{2+} + Fe(CO)_3(PPh_3)_2$$

$$\xrightarrow{\text{acetone}} [Fe(\text{acetone})_x]^{2+} + 2CO\uparrow + PPh_3 \quad (9)$$

The observation of an ESR signal attributable to the intermediate $Fe(CO)_3(PPh_3)_2Cl$ at a considerable time after reaction of $[Fe(CO)_3(PPh_3)_2]^+$ with iron carbonyl complexes and some ligands is also consistent with dimer formation being associated with the reaction scheme. For example, dimers such as $[Rh(CO)_2(PPh_3)_2]_2$ and $[Rh(CO)(PPh_3)_2S]_2$ (S = solvent) react with $CHCl_3$ and CCl_4 to form $RhCl(CO)(PPh_3)_2$ via radical pathways.[20] The work of Connelly et al.[8,11] in conjunction with our studies and oxidative-addition reactions show that reactions of 17-electron radical cations of iron carbonyl compounds may proceed by a number of pathways. Reaction pathways may be parallel, and their characterization is correspondingly difficult.

Acknowledgment. This work was made possible by financial assistance from the Australian Research Grants Committee and the Deakin University Research Committee. We express our gratitude to both these committees for their support.

Registry No. *trans*-$Fe(CO)_3(PPh_3)_2$, 21255-52-7; *trans*-$[Fe(CO)_3(PPh_3)_2]PF_6$, 73979-30-3; $[Fe(CO)_3(PPh_3)_2]^+$, 60243-26-7; $Fe(CO)_4PPh_3$, 35679-07-3; $Fe(CO)_3(AsPh_3)_2$, 20516-72-7; $Fe(CO)_4AsPh_3$, 35644-25-8; $Fe(CO)_3(SbPh_3)_2$, 20516-73-8; $Fe(CO)_4SbPh_3$, 35917-16-9; $Fe(CO)_3(PPh_3)_2Cl$, 73979-38-1; CH_2Cl_2, 75-09-2; Pt, 7440-06-4; Ag, 7440-22-4; Hg, 7439-97-6; PPh_3, 603-35-0; $AsPh_3$, 603-32-7; $SbPh_3$, 603-36-1; acetone, 67-64-1; acetonitrile, 75-05-8.

(20) B. L. Booth, G. C. Casey, and R. N. Haszeldine, *J. Organomet. Chem.*, **224**, 197 (1982).

Contribution from the Department of Chemistry, University of Missouri—Rolla, Rolla, Missouri 65401, Atomic Energy Research Establishment, Harwell, Didcot, OX11 0RA, England, and Inorganic Chemistry and Chemical Crystallography Laboratories, Oxford University, Oxford, OX1 3PD, England

Study of the Iron–Phosphorus–Oxygen System by Mössbauer Effect, Neutron Diffraction, Magnetic Susceptibility, and Analytical Electron Microscopy: Some Pitfalls and Solutions in the Analysis of a Complex Mixture

GARY J. LONG,* ANTHONY K. CHEETHAM, and PETER D. BATTLE*

Received September 27, 1982

A sample of $FePO_4$ has been characterized by powder X-ray and neutron diffraction techniques, Mössbauer spectroscopy, magnetic susceptibility, and analytical electron microscopy. The analysis by diffraction methods is misleading and indicates that the sample is pure, but analytical electron microscopy shows that the material is triphasic and contains, in addition to $FePO_4$, a glassy component of approximate composition $Fe_3P_5O_{17}$ and a small amount of $Fe_7(PO_4)_6$, a mixed valence compound. The Mössbauer-effect spectra indicate that the material contains approximately 30% of the glass and approximately 2% of $Fe_7(PO_4)_6$. The Mössbauer spectra give the expected results for $FePO_4$ and confirm that it orders magnetically at 23.8 K. The glassy component orders at ca. 7 K, whereas $Fe_7(PO_4)_6$ remains paramagnetic down to ca. 10 K. The magnetic susceptibility data show ordering of $FePO_4$ and the glassy component at 24 and ca. 7 K, respectively. The combination of these various techniques has permitted a detailed description of this complex mixture.

Introduction

The discovery of novel ferrimagnetic properties in the isostructural compounds iron(III) sulfate[1] and iron(III) molybdate[2] led us to undertake a detailed study of the magnetic properties of iron(III) phosphate.[3] The latter compound adopts the berlinite ($AlPO_4$) structure,[4] which is related to that of α-quartz with each iron and phosphorus atom tetrahedrally bonded to four oxygen atoms. Prior to our work, little was known about the magnetic nature of iron(III) phosphate. Mössbauer-effect studies[5,6] had indicated that it is antiferromagnetic below ca. 25 K and exhibits a change in the sign of the quadrupole shift at ca. 18 K, but no magnetic susceptibility or neutron diffraction work had been reported. Our study revealed that it undergoes a unique spin-reorientation transition at ca. 17 K.[3]

Our initial measurements were hampered by impurities that were undetected in our characterization of the material by powder X-ray and neutron diffraction, but the combined use of the Mössbauer-effect, analytical electron microscopy, and magnetic susceptibility techniques has allowed us to resolve the detailed nature of the phases present. The purpose of this paper is to discuss the pitfalls that may be encountered when samples are evaluated by diffraction techniques and to describe the experiments that were used to elucidate the actual constituents of the mixture.

Experimental Section

Molten, commercial grade $FePO_4$ (Merck) was held at 1000 °C for 4 h in an open platinum crucible before quenching to room temperature.

The Mössbauer-effect spectra of the ground product were obtained on a Harwell constant-acceleration spectrometer[1] that utilized a room-temperature rhodium-matrix source and was calibrated with room-temperature natural α-iron foil. Spectra obtained at 4.2 K and below were measured in a cryostat in which the sample was placed

*To whom correspondence should be addressed: G.J.L., University of Missouri—Rolla; P.D.B., Oxford University.

(1) Long, G. J.; Longworth, G.; Battle, P.; Cheetham, A. K.; Thundathil, R. V.; Beveridge, D. *Inorg. Chem.* **1979**, *18*, 624.
(2) Battle, P. D.; Cheetham, A. K.; Long, G. J.; Longworth, G. *Inorg. Chem.* **1982**, *21*, 4223.
(3) Battle, P. D.; Cheetham, A. K.; Gleitzer, C.; Harrison, W. T. A.; Long, G. J.; Longworth, G. *J. Phys. C.* **1982**, *15*, L919.
(4) Ng, H. N.; Calvo, C. *Can. J. Chem.* **1975**, *53*, 2064.
(5) Bruckner, W.; Fuchs, W.; Ritter, G. *Phys. Lett. A* **1967**, *26A*, 32.
(6) Beckmann, V.; Bruckner, W.; Fuchs, W.; Ritter, G.; Wegener, H. *Phys. Status Solidi* **1968**, *29*, 781.

0020-1669/83/1322-3012$01.50/0